A Unified Approach for Comprehensive Analysis of Various Spectral and Tissue Doppler Echocardiography

Jiyeon Kim

The Graduate School
Yonsei University
Department of Medical Science

A Unified Approach for Comprehensive Analysis of Various Spectral and Tissue Doppler Echocardiography

A Master's Thesis Submitted
to the Department of Medical Science
and the Graduate School of Yonsei University
in partial fulfillment of the
requirements for the degree of
Master of Medical Engineering

Jiyeon Kim

June 2024

This certifies that the Master's Thesis of Jiyeon Kim is approved.

Thesis Supervisor Hyuk-Jae Chang

정 인현

Thesis Committee Member In-Hyun Jung

이승아

Thesis Committee Member Seung-Ah Lee

The Graduate School
Yonsei University
June 2024

ACKNOWLEDGEMENTS

석사 과정 동안 많은 것을 경험하고 배울 수 있었던 이 귀한 시간을 돌아보며, 저를 지지하고 도와 주신 모든 분들께 진심으로 감사의 말씀을 전합니다.

학위과정 동안 연구함에 있어서 아낌없는 지지하고 지도해주신 장혁재 교수님 그리고 심학준 교수님께 먼저 감사의 인사를 드립니다. 보여주신 열정과 저에게 큰 힘이 되었으며, 앞으로의 길을 나아가는데 큰 힘이 될 것입니다.

함께 공부하며 많은 것을 배울 수 있었던 연구실 분들인 홍영택 소장님, 성민오빠, 영걸오빠, 재익오빠, 경훈오빠, 지나언니, 현석오빠, 가은언니, 주영오빠, 다운언니, 시현에게도 감사 인사를 전합니다. 서로의 경험을 나누며 함께 성장할 수 있었던 시간이 소중하게 남을 것 같습니다. 처음부터 저를 많이 도와준 다운언니, 옆에서 항상 지지해준 시현이에게도 특별한 감사를 전합니다. 무엇보다 제 연구를 이끌어주고 제가 발전할 수 있도록 해준 재익오빠에게 깊이 감사합니다. 함께 연구하면서 새로운 것들을 배울 수 있는 순간이 정말 많았습니다.

마지막으로, 언제나 변함없이 저를 응원해주신 가장 사랑하는 우리 가족에게 감사드립니다. 아낌없이 보내주신 격려가 있었기에 무사히 학위과정을 마칠 수 있었습니다. 언제나 사랑하고 감사합니다.

김지연 드림

TABLE OF CONTENTS

LIST OF FIGURES

LIST OF TABLES

ABSTRACT

A Unified Approach for Comprehensive Analysis of Various Spectral and Tissue Doppler Echocardiography

Doppler echocardiography offers critical insights into cardiac function and phases by quantifying blood flow velocities and evaluating myocardial motion. However, previous methods for automating Doppler analysis, ranging from initial signal processing techniques to advanced deep learning approaches, have been constrained by their reliance on electrocardiogram (ECG) data and their inability to process Doppler views collectively. We introduce a novel unified framework using a convolutional neural network for comprehensive analysis of spectral and tissue Doppler echocardiography images that combines automatic measurements and end-diastole (ED) detection into a singular method. The network automatically recognizes key features across various Doppler views, with novel Doppler shape embedding and anti-aliasing modules enhancing interpretation and ensuring consistent analysis. Empirical results indicate a consistent outperformance in performance metrics, including dice similarity coefficients (DSC) and intersection over union (IoU). The proposed framework demonstrates strong agreement with clinicians in Doppler automatic measurements and competitive performance in ED detection.

Key words : doppler imaging, deep learning, end-diastole detection, automatic measurement

1. Introduction

Doppler echocardiography is pivotal in assessing cardiac function, particularly through its ability to capture dynamic, time-dependent changes in velocity. Spectral Doppler effectively maps the velocity and direction of blood flow over time, while Tissue Doppler Imaging (TDI) is adept at measuring the time-variant velocity of myocardial tissue. These modalities, through the analysis of spectral and tissue Doppler imaging, provide critical clinical metrics, including maximum blood flow velocity (Vmax) and velocity time integral (VTI). Importantly, the full spectrum of data these techniques offer extends well beyond these commonly measured indicators, capturing a comprehensive temporal dynamics of cardiac cycles.

Since early works, efforts to automatically measure clinical parameters from Doppler images have been made. These approaches [1, 2, 3] primarily relied on digital and signal processing, involving steps such as noise filtering to obtain the Doppler envelope and thresholding to detect key points for obtaining clinical measurements. Nonetheless, these algorithms were often compromised by poor contrast and image artifacts, and required hyperparameter tuning for each views, making them less effective and creating significant challenges for comprehensive automated Doppler analysis.

Recent deep learning-based methods have advanced the analysis of Doppler images, notably improving the classification of Doppler types [4, 5], the evaluation of Doppler flow quality [6], and the automation of mitral inflow velocity measurements [7]. Nevertheless, these methods depend on electrocardiograms (ECG) for determining cardiac phases or identifying regions of interest, and are restricted to processing each Doppler view individually. The continued dependence on ECG and the view-specific limitation indicate only modest progress. Despite efforts to automatically detect end-diastole (ED) [8], full integration with automated measurement is lacking. This gap highlights the pressing need for a unified framework that would bring together all aspects of Doppler echocardiography analysis. Such a framework would not only facilitate cardiac phase recognition and extensive automatic measurement across the full spectrum of Doppler views but also achieve this without the need for ECG or other auxiliary inputs.

In this work, we present a novel unified framework that enables comprehensive analysis of various spectral and tissue Doppler echocardiography images using a single fully convolutional network (Figure 1). To equip the network to discern the temporal dynamics of cardiac cycles without ECG, we have trained the segmentation network using annotated segmentation masks that mimic the VTI. This segmentation is pivotal; it not only captures key topological features for clinical measurement but also integrates information on the cardiac phase, given that VTI is characterized as the integral of the velocity curve over a cardiac cycle. Our single network is trained on a comprehensive dataset that covers the full spectrum of Doppler modalities, including both pulsed wave (PW) and continuous wave (CW) Doppler, as well as extending to TDI, thus enabling it to autonomously learn and discern key features across these varied views. To effectively support an integrated interpretation of diverse Doppler signal data, we propose a Doppler shape embedding module. Additionally, we propose the integration of an anti-aliasing module to ensure baseline-shift equivariance, which is essential for maintaining consistent analysis despite variations in baseline positioning. Our tailored modules demonstrate consistent performance increases compared to networks without these enhancements in metrics such as Dice similarity coefficients (DSC) and

Intersection over union (IoU). Our comprehensive approach not only excels in automatic measurements and ED detection but also sets a new standard by eliminating the need for ECG data, a significant step beyond previous ECG-dependent and single-view methods.

2. Methods

In the section, we provide a detailed description of the segmentation network, which incorporates the Doppler shape embedding module alongside an anti-aliasing strategy. We will then outline the methodology for extracting clinical parameters, such as Vmax and VTI. Moreover, we will present a clinical application: a method for detecting ED.

2.1. Doppler envelope segmentation

The segmentation architecture is reinforced by two key modules: a Doppler Shape Embedding module and an antialiasing module, each tailored to overcome distinct challenges in interpreting Doppler signals.

The Doppler shape embedding module, inspired by insights from prior research [9], is designed to capture the shape features intrinsic to Doppler spectrograms for each Doppler view. As depicted in Figure 1, Doppler signals can be classified into seven distinct flow types based on valve positions and the direction of blood flow – whether anterograde or retrograde. Accordingly, the shape embedding block is strategically designed to incorporate this contextual knowledge, particularly at the final stage of the encoder, possessing high-level semantic details. This module, situated at the encoder's final stage, applies global average pooling followed by a 1×1 convolution, enhancing the semantic features related to Doppler shapes. This integration of contextual knowledge, along with a shape head for signal pattern classification and correction via context loss, ensures precise feature weighting corresponding to the diverse Doppler signals.

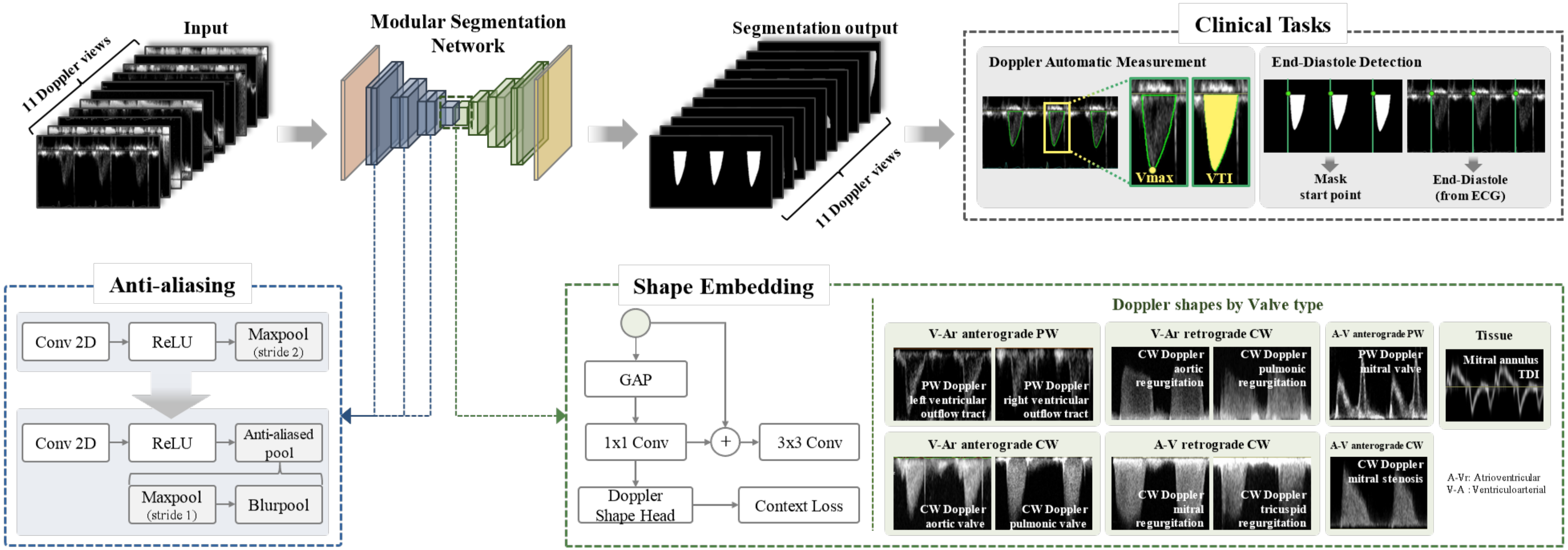

Figure 1. Unified framework for comprehensive analysis. The network, with its anti-aliasing and Doppler shape embedding modules, accurately processes diverse Doppler views and supports clinical tasks like automatic measurement and ED detection. Doppler shape embedding module integrates shape-specific features through global average pooling and 1×1 convolution at the encoder's final stage, enhancing the network's ability to accurately classify and analyze diverse Doppler signal shapes. Anti-aliasing module reduces sensitivity to small positional or scale changes in input Doppler signals, ensuring consistent and reliable outputs. By this modules, the segmentation network automates the extraction of clinical parameters from Doppler, and detects end-diastole using direct observations of blood flow changes. This framework can result in multiple clinical tasks with single deep learning network.

The anti-aliasing module tackles the issue of baseline shift. Clinicians often adjusts the Doppler signals' vertical position to better visualize regions of interest (e.g., dominant flow), as shown in Figure 2. However, a recent study [10] reports that small input translations or rescaling significantly affect modern network's prediction. By incorporating an antialiasing strategy, our network maintains robust performance, producing consistent segmentations even when the Doppler signal is manually adjusted, thus optimizing the utility of echocardiographic analysis in clinical practice. In this paper, we use Blurpool, proposed in [11], as our anti-aliasing strategy. Blurpool consists of two operations: blurring filter with kernel $k \times k$ and subsampling. Therefore, we replace every max-pooling and a strided convolution operation with Blurpool, enabling the segmentation model to be anti-aliased and have a consistent output for baseline shift.

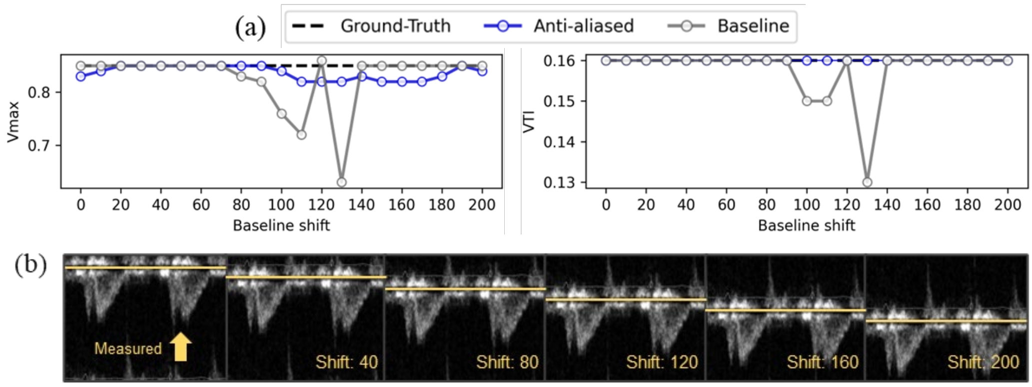

Figure 2. Performance comparison with and without the anti-aliasing module, against baseline shifts. (a) Performance comparison in Doppler auto-measurements ($\boldsymbol{V_{max}}$ **and** $\boldsymbol{VTI}$). (b) Baseline shifts in Doppler imaging ranging from baseline to 200. Following shifts corresponds to x-axis in (a).

The total network optimization loss, L_{total}, combines segmentation loss, L_{seg}, and context loss, $L_{context}$, weighted by a factor μ, and is defined as $L_{total} = L_{seg} + \mu L_{context}$, with both losses calculated via cross-entropy.

2.2. Modular Segmentation Networks

Our framework's modularity facilitates the seamless integration of Doppler Shape Embedding and anti-aliasing modules into any existing encoder-decoder based convolutional architectures. To evaluate our approach, we engaged in comparative analyses with renowned segmentation networks, including Unet [12], UNet++ [13], and BiSeNetV2 [9].

2.3. Clinical Parameters Computation and ED detection

Given our segmentation network's training protocol, acquiring clinical parameters becomes remarkably straightforward. Once we obtain the segmentation mask, the VTI measurement naturally falls into place. This mask diligently pinpoints velocity profiles within our designated regions of interest, using the baseline for contextual reference. The maximum velocity is then measured by identifying the pixel positioned at the greatest distance from this baseline within the segmented Doppler signal.

In our approach, the detection of ED is based on the observation of blood flow initiation or termination. For instance, in PW or CW Doppler of the atrioventricular (A-V) valves (mitral or tricuspid valve), the termination of anterograde flow indicates the closure of the A-V valve, delineating the ED, a detail that our Doppler envelope segmentation clearly capture. Similarly, the initiation of anterograde flow in PW or CW Doppler across ventriculoarterial (V-Ar) valves (aortic or pulmonic valve) marks the beginning of ventricular systole and simultaneously denotes the ED. Traditional methods, like those seen in [8], determine these critical phases using the R-peak from ECG data. However, our method offers a more direct and potentially precise way to determine these events means of identifying these events by directly utilizing the timing of valve movements. A comprehensive breakdown of how the start or end of flow in specific views determines the ED can be found in Table 2.

3. Experiments and Results

Our research employed a dataset of 25,854 Doppler DICOM files from 6,854 patients provided by the OpenAI Dataset Project (AI-Hub), a South Korean Ministry of Science and ICT initiative [14]. In collaboration with clinicians, 11 clinically-relevant views were selected based on the ASE guidelines. Sonographers annotated segmentation masks for training and validating our network, which were also used to derive clinical parameters such as Vmax and VTI. ED labeling for ED detection performance evaluation was initially automated using the R-peak detection algorithm from ECG with subsequent manual verification. The data was split at the patient level into training (80%), validation (10%), and testing (10%) sets. Employing the Monte Carlo cross-validation method, we repeated the dataset split five times to thoroughly evaluate our model's segmentation accuracy. For the segmentation performance, we report the average values derived from multiple dataset splits, and for the evaluation of Doppler measurements and end-diastole (ED) detection, we present the results from the first split of the test set.

3.1. Implementation Details

Our experiments were carried out using PyTorch. Doppler envelope is cropped from the original Dicom image using the header information (tag 0018, 6011), and resized to 256×512. Inputs were resized to the same value in the validation and test phase, preserving the original ratio. All image values were scaled between -1 and 1. No additional augmentations were used. The segmentation networks were trained using the Adam optimizer with learning rate of 1e-3. Both the proposed and comparison methods are trained for 200 epochs with a batch size of 32 and early stopped training when the validation segmentation loss stops improving.

3.2. Doppler Envelope segmentation

The effectiveness of our proposed modules on segmentation performance was assessed using DSC and IoU. Table 1 displays the comparison between our enhanced models with proposed modules and baseline models, showing that our modules consistently outperforms network performance. The improvements are particularly noticeable in CW Doppler, with metrics like DSC and IoU consistently higher. This indicates that our Doppler shape embedding module, which integrates shape context, is key to extracting semantically rich features.

Furthermore, Figure 2 shows that incorporating the antialiasing module effectively counters baseline-shifts, maintaining automatic measurement performance. The absence of the anti-aliasing module results in significant discrepancies in both Vmax and VTI whenever baseline shifts occur. In contrast, the application of BlurPool demonstrates a notable reduction in deviations from the GT, yielding more consistent outputs. This outcome underscores the module's efficacy and validates its capacity to faithfully capture and reflect the inherent traits and variations present in Doppler images.

Table 1 Comparative performance analysis across three different modalities

Module	Mode	UNet		UNet++		BiSeNetV2	
		Vanilla	Anti-aliasing + Shape Embedding	Vanilla	Anti-aliasing + Shape Embedding	Vanilla	Anti-aliasing + Shape Embedding
mDice	PW	0.931	**0.934**	0.933	**0.934**	0.931	**0.932**
	CW	0.921	**0.926**	0.925	**0.927**	0.923	**0.924**
	TDI	0.914	**0.915**	0.916	**0.917**	0.909	**0.912**
mIoU	PW	0.876	**0.880**	0.879	**0.882**	0.876	**0.878**
	CW	0.870	**0.877**	0.876	**0.879**	0.873	**0.875**
	TDI	0.845	**0.846**	0.848	**0.849**	0.836	**0.841**
Total (mDice)		0.922	**0.925**	0.925	**0.926**	0.921	**0.923**
Total (mIoU)		0.863	**0.868**	0.868	**0.870**	0.862	**0.865**

3.3. Clinical Tasks

3.3.1 Automatic Measurements

We employed Pearson correlation coefficients (PCC) to determine the agreement with clinicians. Ground truth (GT) segmentation masks serve as the basis for extracting these clinical measurements. The PCC was calculated by matching cardiac beats between the GT and the predictions, and the true detection rate ($TDR_{measure}$) was assessed by the ratio of number of correctly matched predictions to the GT count.

In Table 2, a consistent and notably high correlation was observed for Vmax and VTI across all views. Figure 3 (a) further illustrates this trend through a scatter plot, highlighting the outstanding agreement between the model and clinician.

3.3.2 End-diastole Detection

For ED detection performance, a detection limit parameter λ was set , classifying predictions as accurate if the estimated ED fell within λ of the R-peak in the ECG. The TDR_{ED}, defined as the ratio of correctly detected EDs to the entire count of labeled EDs, was then calculated, excluding the EDs within 100ms of boundaries, aligning with the evaluation presented in [8].

Table 2 Summary of automatic measurement correlations and end-diastole detection rates across various Doppler views

Valve type	View	# Images	# Beats	Clinical Measurements		
				$Vmax$ (PCC)	VTI (PCC)	$TDR_{measure}$ (%)
V-Ar anterograde PW	PW Doppler LVOT	246	756	0.952	0.916	99.34
	PW Doppler RVOT	294	856	0.971	0.930	97.72
V-Ar anterograde CW	CW Doppler AS	295	911	0.989	0.981	99.02
	CW Doppler PS	19	76	0.958	0.953	97.44
A-V anterograde PW	MV inflow PW	417	1,105	0.982	-	98.05
A-V anterograde CW	CW Doppler MS	125	354	0.963	0.976	99.16
V-Ar retrograde CW	CW Doppler AR	97	280	0.972	-	99.65
	CW Doppler PR	14	41	0.984	-	97.62
A-V retrograde CW	CW Doppler MR	129	366	0.965	0.956	99.73
	CW Doppler TR	467	1,210	0.961	0.940	98.45
Tissue	Septal annulus TDI	405	1,436	0.916	-	98.09
Total		**2,508**	**7,391**	**0.9648**	**0.9504**	**98.52**

A-V: Atrioventricular; V-Ar: ventriculoarterial; E', A', S' for TDI and E, A for MV inflow in Vmax.

We present results obtained with the parameter λ at 0.08sec in Table 2. The data overall are quite promising. Particularly, examining PW or CW Doppler of A-V valves (mitral or tricuspid valve), we observe TDR_{ED} approaching 100%. This aligns with the theoretical expectations for ED detection. On the other hand, we observe a decrease in the accuracy of ED detection in the context of CW Doppler of V-Ar valve (aortic or pulmonic valve) regurgitation. This can be attributed to the characteristic prolongation of regurgitant flow through the V-Ar valve, which extends beyond the ED phase and into the isovolumic contraction time. Figure 3 (b) provides a graphical representation of TDR_{ED} as a function of λ, offering insights into sensitivity. This visual aid helps us understand the variations in TDR based on different λ values.

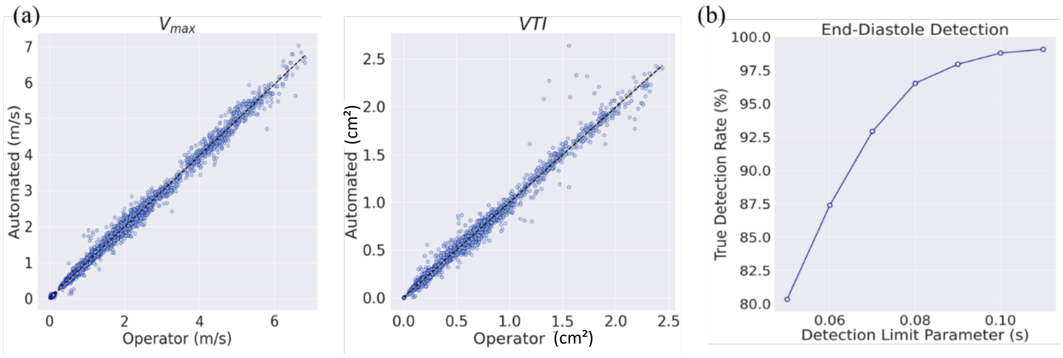

Figure 3. Clinical correlation plots and TDR curve for ED detection. (a) Scatter plots display strong correlations between Vmax and VTI predictions with clinician assessments. (b) A curve shows the model's TDR for ED across different λ thresholds.

4. Conclusion

Our study presents a unified framework for analyzing spectral and tissue Doppler echocardiography images, enabling automatic measurements and cardiac phase detection without relying on electrocardiogram (ECG) data. Our method measures 11 types of Doppler views across three modes, using a convolutional neural network (CNN) for automatic measurements and end-diastole (ED) detection. The framework includes a Doppler shape embedding module and an anti-aliasing strategy, ensuring accurate processing of diverse Doppler views.

Results show our approach outperforms existing methods in key performance metrics like dice similarity coefficients (DSC) and intersection over union (IoU). High Pearson correlation coefficients (PCC) for clinical parameters, such as maximum blood flow velocity (Vmax) and velocity time integral (VTI), indicate strong agreement with clinicians. The method also maintains high true detection rates (TDR) for ED across various Doppler views, crucial for accurate cardiac phase recognition.

Future work will focus on enhancing measurement capabilities, particularly for time parameters, and conducting external validations to confirm efficacy across different patient populations and clinical settings. Additionally, we aim to extend our system to detect end-systole, enhancing the clinical utility of automated Doppler echocardiography analysis.

References

[1] JinHyeong Park, S Kevin Zhou, John Jackson, and Dorin Comaniciu, "Automatic mitral valve inflow measurements from doppler echocardiography," in International Conference on Medical Image Computing and Computer-Assisted Intervention. Springer, 2008, pp. 983–990.

[2] Massoud Zolgharni, Niti M Dhutia, Graham D Cole, M Reza Bahmanyar, Siana Jones, SM Afzal Sohaib et al, "Automated aortic doppler flow tracing for reproducible research and clinical measurements," IEEE transactions on medical imaging, vol. 33, no. 5, pp. 1071–1082, 2014.

[3] Amirtah`a Taebi, Richard H Sandler, Bahram Kakavand, and Hansen A Mansy, "Estimating peak velocity profiles from doppler echocardiography using digital image processing," in 2018 IEEE signal processing in medicine and biology symposium (SPMB). IEEE, 2018, pp. 1–4.

[4] Eleonora Sulas, Emanuele Ortu, Luigi Raffo, Monica Urru, Roberto Tumbarello, and Danilo Pani, "Automatic recognition of complete atrioventricular activity in fetal pulsed-wave doppler signals," in 2018 40th Annual International Conference of the IEEE Engineering in Medicine and Biology Society (EMBC). IEEE, 2018, pp. 917–920.

[5] Andrew Gilbert, Marit Holden, Line Eikvil, Mariia Rakhmail, Aleksandar Babi´c, Svein Arne Aase et al, "User-intended doppler measurement type prediction combining cnns with smart post-processing," IEEE journal of biomedical and health informatics, vol. 25, no. 6, pp. 2113–2124, 2020.

[6] Ghada Zamzmi, Li-Yueh Hsu, Wen Li, Vandana Sachdev, and Sameer Antani, "Echo doppler flow classification and goodness assessment with convolutional neural networks," in 2019 18th IEEE International Conference On Machine Learning And Applications (ICMLA). IEEE, 2019, pp. 1744–1749.

[7] Mohamed Y Elwazir, Zeynettin Akkus, Didem Oguz, Zi Ye, and Jae K Oh, "Fully automated mitral inflow doppler analysis using deep learning," in 2020 IEEE 20th International Conference on Bioinformatics and Bioengineering (BIBE). IEEE, 2020, pp. 691–696.

[8] Tollef Struksnes Jahren, Erik N Steen, Svein Arne Aase, and Anne H Schistad Solberg, "Estimation of end-diastole in cardiac spectral doppler using deep learning," IEEE Transactions on Ultrasonics, Ferroelectrics, and Frequency Control, vol. 67, no. 12, pp. 2605–2614, 2020.

[9] Changqian Yu, Changxin Gao, Jingbo Wang, Gang Yu, Chunhua Shen, and Nong Sang, "Bisenet v2: Bilateral network with guided aggregation for real-time semantic segmentation," International Journal of Computer Vision, vol. 129, pp. 3051–3068, 2021.

[10] Xueyan Zou, Fanyi Xiao, Zhiding Yu, Yuheng Li, and Yong Jae Lee, "Delving deeper into anti-aliasing in convnets," International Journal of Computer Vision, vol. 131, no. 1, pp. 67–81, 2023.

[11] Richard Zhang, "Making convolutional networks shift-invariant again," in International conference on machine learning. PMLR, 2019, pp. 7324–7334.

[12] Olaf Ronneberger, Philipp Fischer, and Thomas Brox, "U-net: Convolutional networks for biomedical image segmentation," in Medical Image Computing and Computer-Assisted Intervention–MICCAI 2015: 18th International Conference, Munich, Germany, October 5-9, 2015, Proceedings, Part III 18. Springer, 2015, pp. 234–241.

[13] Zongwei Zhou, Md Mahfuzur Rahman Siddiquee, Nima Tajbakhsh, and Jianming Liang, "Unet++: A nested unet architecture for medical image segmentation," in Deep Learning in Medical Image Analysis and Multimodal Learning for Clinical Decision Support: 4th International Workshop, DLMIA 2018, and 8th International Workshop, ML-CDS 2018, Held in Conjunction with MICCAI 2018, Granada, Spain, September 20, 2018, Proceedings 4. Springer, 2018, pp. 3–11.

[14] AI-Hub,
https://aihub.or.kr/aihubdata/data/view.do ?currMenu=115&topMenu=&aihubDataSe=data&dataSetSn =502.

Abstract in Korean

다양한 스펙트럴 및 조직 도플러 심장초음파의 체계적 분석을 위한 통합적 접근 방법

도플러 심초음파는 혈류 속도를 정량화하고 심근 운동을 평가함으로써 심장 기능과 단계를 분석하는 데 중요한 통찰을 제공함. 그러나 기존의 도플러 분석 자동화 방법은 초기 신호 처리 기술에서부터 딥러닝 접근법에 이르기까지 심전도(ECG) 데이터에 대한 의존성과 도플러 뷰를 통합적으로 처리하지 못하는 한계가 있었음. 본 연구에서는 스펙트럼 및 조직 도플러 심초음파 영상을 종합적으로 분석하기 위해 컨볼루션 신경망(CNN)을 사용하는 새로운 통합 프레임워크를 도입함. 이 프레임워크는 자동 측정과 말기 이완기(ED) 검출을 하나의 방법으로 결합함. 네트워크는 다양한 도플러 뷰에서 주요 특징을 자동으로 인식하며, 도플러의 형태적 특징 기반 임베딩 및 안티앨리어싱(Anti-aliasing) 모듈을 통해 해석을 강화하고 일관된 분석을 보장함. 실험 결과에 따르면 제안된 프레임워크는 다이스 유사 계수(DSC) 및 교차 영역 합집합(IoU)과 같은 성능 지표에서 일관된 우수성을 나타냄. 또한, 제안된 프레임워크는 도플러 자동 측정에서 임상의의 측정 값과 높은 상관관계를 보이며, ED 검출에서도 경쟁력 있는 성능을 보임.

핵심되는 말 : 도플러 영상, 딥러닝, 말기 이완기 검출, 자동 측정